

AD-778 660

APPROXIMATIONS TO THE DIRECTIVITY
INDEX

Robert J. Bobber

Naval Research Laboratory
Washington, D. C.

1 May 1974

DISTRIBUTED BY:

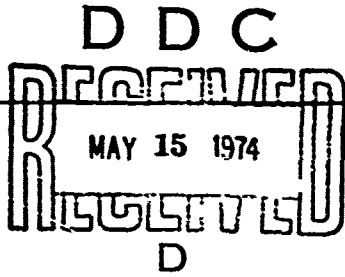
NTIS

National Technical Information Service
U. S. DEPARTMENT OF COMMERCE
5285 Port Royal Road, Springfield Va. 22151

UNCLASSIFIED

SECURITY CLASSIFICATION OF THIS PAGE (When Data Entered)

AD 778 660

REPORT DOCUMENTATION PAGE		READ INSTRUCTIONS BEFORE COMPLETING FORM
1. REPORT NUMBER NRL Report 7750	2. GOVT ACCESSION NO.	3. RECIPIENT'S CATALOG NUMBER
4. TITLE (and Subtitle) APPROXIMATIONS TO THE DIRECTIVITY INDEX		5. TYPE OF REPORT & PERIOD COVERED Final report on one part of the problem
7. AUTHOR(s) Robert J. Bobber		6. PERFORMING ORG. REPORT NUMBER
3. PERFORMING ORGANIZATION NAME AND ADDRESS Naval Research Laboratory Underwater Sound Reference Division F.O. Box 8337, Orlando, FL 32806		8. CONTRACT OR GRANT NUMBER(s)
11. CONTROLLING OFFICE NAME AND ADDRESS Department of the Navy Office of Naval Research Arlington, VA 22217		10. PROGRAM ELEMENT, PROJECT, TASK AREA & WORK UNIT NUMBERS NRL Problem K03-30.401
14. MONITORING AGENCY NAME & ADDRESS (if different from Controlling Office)		12. REPORT DATE 1 May 1974
		13. NUMBER OF PAGES iii + 17
		15. SECURITY CLASS. (of this report) UNCLASSIFIED
		15a. DECLASSIFICATION/DOWNGRADING SCHEDULE
16. DISTRIBUTION STATEMENT (of this Report) Approved for public release; distribution unlimited		
17. DISTRIBUTION STATEMENT (of the abstract entered in Block 20, if different from Report)		
18. SUPPLEMENTARY NOTES		
19. KEY WORDS (Continue on reverse side if necessary and identify by block number) Directivity index Underwater sound transducers		
Reproduced by NATIONAL TECHNICAL INFORMATION SERVICE U S Department of Commerce Springfield VA 22151		
20. ABSTRACT (Continue on reverse side if necessary and identify by block number) Directivity indexes of three different underwater sound transducers have been measured or computed by five different methods: (1) theoretical calculations using piston area or line length, (2) beam-width measurement and theoretical calculation, (3) pattern measurement and graphical integration, (4) direct digital directivity index measuring system, and (5) diffuse-sound method. The results indicate that the directivity index of any ordinary transducer can be obtained from calculations based on known configurations and dimensions or		

DD FORM 1 JAN 73 7473

EDITION OF 1 NOV 65 IS OBSOLETE
S/N 0102-014-6601

i

UNCLASSIFIED

SECURITY CLASSIFICATION OF THIS PAGE (When Data Entered)

20. Abstract (continued)

- beam-width measurements with a degree of reliability and accuracy that is no worse than any measurement technique and that, in most cases, elaborate measurements for determining directivity index are not justified.

Contents

Introduction	1
Comparison of Five Methods	1
Energy in Minor Lobes	4
Circular Pistons	5
Rectangular and Other Pistons	7
Radiating Areas	8
Beam Widths	9
Rear Lobes	9
Radiation Resistance	10
Line Sources	11
Shaded Transducers	13
Arrays with Mutual Coupling	15
Conclusion	16
Acknowledgement	16
References	16

Figures

1. Array configurations for (a) one quadrant of type F27 transducer, (b) one quadrant of type F33 transducer, and (c) type F37 line transducer	2
2. The directivity index of (a) type F27 transducer, (b) type F33 transducer, and (c) type F37 transducer, as determined by methods 1, 2, 3, 4, and 5	4
3. The directivity index of a circular piston of diameter d without baffle, with a rigid plane baffle, in the end of an infinitely long rigid pipe, and as approximated by the expression $10 \log (4\pi A/\lambda^2)$	6
4. The directivity index of a rectangular piston in an infinite plane rigid baffle as a function of length L or width W	7
5. The directivity index of a line source according to Stenzel's exact expression (Eq. (8)), and three degrees of approximation by Eq. (10)	12
6. Major lobes of patterns for a uniform line, a linearly tapered line, and 10-element binomially shaded line array	15

Tables

1. Percentage of acoustic energy in each lobe of an ideal piston with a diameter of d/λ wavelengths, and an ideal line with a length of L/λ wavelengths	5
2. Correction (in decibels) to calculated directivity index as a function of rear lobe height	10

APPROXIMATIONS TO THE DIRECTIVITY INDEX

Introduction

The directivity index has long been an important parameter in evaluating some types of electroacoustic transducers--particularly in sonar applications. It is a difficult parameter to analyze and measure because a three-dimensional integration of the radiation pattern is involved. For this reason, approximations have been widely used in both the theory and measurement. In spite of the fact that Stenzel [1], Molloy [2], and others worked out the fundamental theory many years ago, there has been little quantitative analysis of the theoretical and measurement approximations. At the same time, transducer designers have either gone to elaborate and costly techniques to measure the directivity index [3-8], or have used very simple computational aids such as special slide rules that are based on idealized models [9]. The purpose of this study was to compare the results of these two extremes in methodology, to quantify some of the limits of approximations, to identify the most feasible method of determining the directivity index, and to report some results of two little known or used measurement methods. An unexpected side light has been the identification of an error in Stenzel's original analysis and some errors in translating Stenzel's work into English [10,11] and in preparing a second edition of his book [12].

The principal conclusion from this study was that, in most cases, elaborate measurements for determining the directivity index are not justified by the accuracy or precision of the results.

Comparison of Five Methods

Directivity factors of three different underwater sound transducers have been measured or computed by five different methods.

The three transducers are NRL-USRD types F27, F33, and F37. The F27 approximates a uniform circular piston in a rigid baffle, as shown in Fig. 1a. It is comprised of an array of 55 lead metaniobate disks. The type F33 approximates a nonuniform circular piston in a rigid baffle, as shown in Fig. 1b. It is comprised of two arrays. The outer array contains 64 barium titanate rectangular plates; the inner array, 12 lead

zirconate circular disks. The transducer was designed with the dual configuration to provide a wide useful frequency range. For the experiments described here, the two arrays were electrically connected and used as one array. The type F37 approximates a uniform line, or thin cylinder, as shown in Fig. 1c. It is comprised of a line of eight lead zirconate capped cylinders.

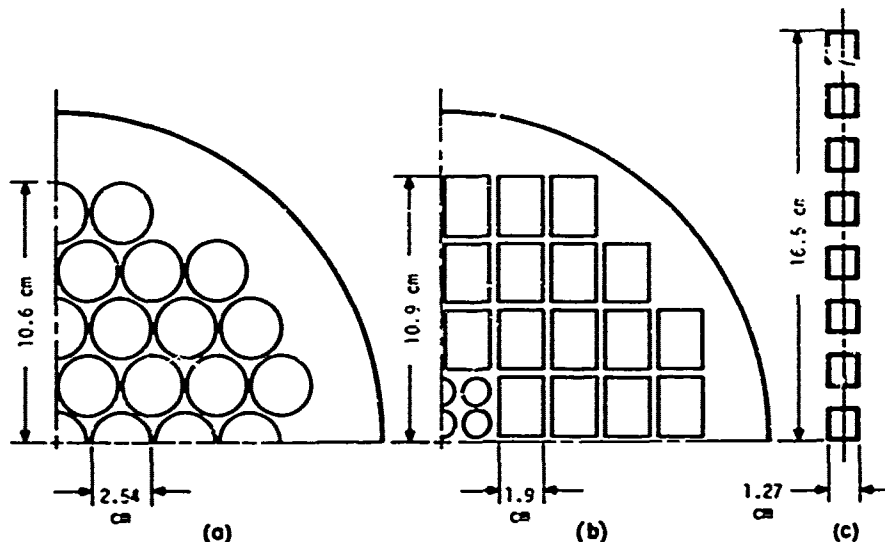


Fig. 1. Array configurations for (a) one quadrant of type F27 transducer, (b) one quadrant of type F33 transducer, and (c) type F37 line transducer.

The five methods are:

1. *Theoretical Calculations Using Piston Area or Line Length.* This method requires only theoretical calculations based on well-known approximations. The directivity factor of a piston in an infinite rigid baffle is given approximately by the expression $4\pi A/\lambda^2$, where A is the piston area and λ is the wavelength. For a line or thin cylinder, the corresponding expression is $2L/\lambda$, where L is the length. These are simple expressions, but uncertainties usually arise in ascertaining A and L because, in practice, both pistons and lines are really arrays of elements. The spaces between the elements usually are included in A and L , but the effective edges or ends of the arrays are more indefinite, and generally introduce an uncertainty of about 5% for L and 10% for A .

2. *Beam-Width Measurement and Theoretical Calculation.* The beam width of the radiation pattern was measured. The transducer size and shape were inferred from these measurements, and the directivity factor then was calculated in a manner similar to the first method. In both calculation methods, it is assumed that the differences between the theoretical and real minor lobe structures in the pattern are negligible.

3. *Pattern Measurement and Graphical Integration.* A number of two-dimensional patterns were plotted. Then graphical integrations were carried out to ascertain approximately the three-dimensional pattern. This is a standard method, but very time consuming unless the pattern has circular symmetry about at least one axis, or some computerized technique [4,5] is used for the integration.

4. *Direct Digital Directivity Index Measuring System.* A new digital system was used [6,7]. A seven-element semicircular hydrophone array was swept through a spherical surface around the transducer, and 252 samples of the radiated sound pressure level were obtained in a few minutes. The 252 values were processed by digital computer methods to obtain the directivity factor in a short time. No patterns, *per se*, are required for this method.

5. *Diffuse-Sound Method.* The identity between the directivity factor and the ratio of the free-field to the diffuse-field receiving sensitivity of a transducer [13] was used. Diffuse fields or reverberent chambers have been little used in underwater acoustics because of the long wavelengths and difficulties in obtaining large impedances mismatches. The diffuse field sensitivities used in this experiment were obtained by B. G. Watters in the reverberation tank at the Bolt, Beranek, and Newman company in Cambridge, Mass. [14]. This tank has the dimensions 9.75 x 7.01 x 4.27 meters and reverberation times as long as 5 seconds. The only other reported use of this method is from Reznikov and Snytko [15] who used both spatial and temporal averaging in a small water-filled vessel. Their work is difficult to assess or use because of an incomplete description of the transducer, the use of unexplained corrections, and results which show that the directivity factor of a cylindrical transducer is not proportional to frequency, as it should be.

The directivity index, or ten times the logarithm of the directivity factor, is shown in Fig. 2 for the three transducers as determined by the five methods. The calculated directivity indexes for the types F27 and F33 from the first method are shown as broad lines, 0.5 dB wide, because of the uncertainty in the value to be used for the area A.

The agreement among all methods except the fifth (diffuse field) is unusually good for the F33--so good that all data points fall within the 0.5-dB spread of the calculated values. The diffuse field data are clearly too high. The discrepancy probably is due to the imperfect diffuseness of the field.

The scatter among the methods is greater for the F27, but the average of the three experimental methods (3, 4, and 5) agrees well with the two calculation methods (1 and 2).

For the F37, four of the five methods are in good agreement above 20 kHz, but this time it is the digital method that does not agree; however, only one (25 kHz) of the three data points is widely different. Below 20 kHz the diffuse field method is again too high.

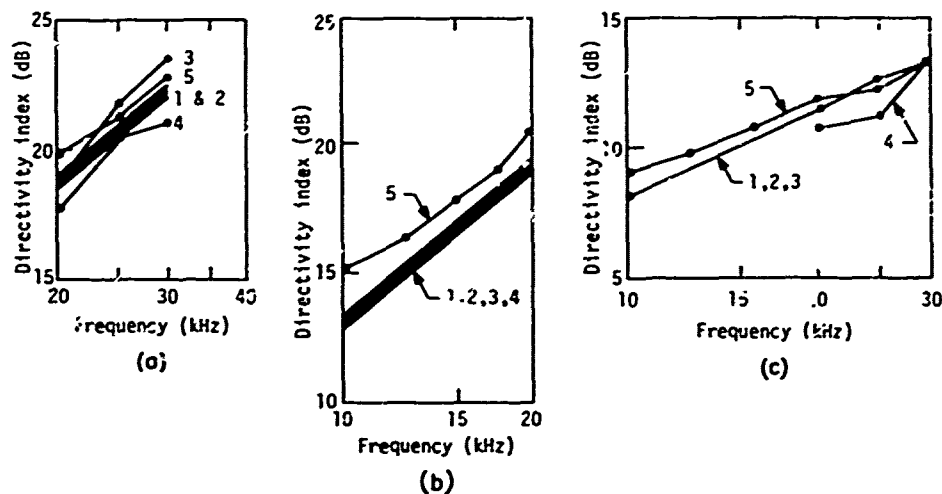


Fig. 2. The directivity index of (a) type F27 transducer, (b) type F33 transducer, and (c) type F37 transducer, as determined by methods 1, 2, 3, 4, and 5.

The data show that the diffuse-field method in the BBN tank should be limited to 25 kHz and higher frequencies. Beyond that, there is not sufficient consistency in the data to conclude that one of the three experimental methods is to be preferred.

The one conclusion that emerges from the experiment is that the directivity index obtained from the theoretical or from the beam width calculations is as reliable as any of the experimental methods, and it appears futile to go to elaborate measurements for transducers of conventional shapes.

Energy in Minor Lobes

Table 1 shows the acoustic energy distribution among the major and minor lobes in typical patterns. It is evident from this table that minor lobes contribute very little to the directivity factor or index. Neglecting all the minor lobes would introduce an error of less than 0.8 dB for a piston and less than 0.4 dB for a line. In practice, of course, it is not a matter of entirely neglecting the minor lobes, but rather neglecting the difference between the idealized and the real pattern. Clearly, 1- or 2-dB variations in the height of the first minor lobe and even larger variations in the others are not going to make perceptible differences between the real directivity index and the directivity index based on an ideal model and measurements of only the major lobe. This fact, of course, supports the thesis that once the beam width of the major lobe is known, along with the basic configuration of the radiator (circle, rectangle, cylinder, etc.), and the knowledge that the minor lobe structure is not radically abnormal, no further measurement is necessary.

Table 1. Percentage of acoustic energy in each lobe of an ideal piston with a diameter of d/λ wavelengths, and an ideal line with a length of L/λ wavelengths.

d/λ	L/λ	Major Lobe	Minor Lobes							
			1	2	3	4	5	6	7	
2		0.85	0.15							
3		.84	.09	0.07						
5		.84	.08	.03	0.02	0.03				
8		.84	.08	.03	.02	.01	0.00	0.00	0.02	
	2	0.95	0.05							
	3	.93	.05	0.02						
	5	.92	.05	.02	0.01	0.00				
	8	.92	.05	.01	.01	.00	0.00	0.00	0.00	

An interesting side light is shown in Table 1. The energy in successive side lobes does not always diminish steadily. In large pistons the last minor lobe contains more energy than some intermediate lobes. The larger solid angle of the last lobe more than compensates for the lower average level.

Circular Pistons

After one is persuaded that calculations based on approximations are sufficient in most cases to determine the directivity index, it is still necessary to define quantitative limits for these approximations. Of the common configurations, the circular piston in a rigid plane baffle is the best known. Figure 3 shows the directivity index D_i for the rigorous case computed from

$$D_i = 10 \log \left(\frac{(kd/2)^2}{1 - \frac{2J_1(kd)}{kd}} \right), \quad (1)$$

where $k = 2\pi/\lambda$, d is the diameter of the piston, and J_1 denotes the first-order Bessel function, and for the approximation based on the area,

$$D_i = 10 \log (4\pi A/\lambda^2). \quad (2)$$

It also shows the directivity index from Beranek [16] for the two most common departures from an infinite plane rigid baffle. Many underwater sound transducers approximate the piston in the end of a long tube. An unbaffled loudspeaker is an example of the unbaffled piston, which approximates a dipole with a directivity index of 4.7 dB at low frequencies and is consistently 3 dB lower than the baffled piston at high frequencies because of its bidirectional pattern. At high frequencies, it is the same as a plane baffled piston radiating in both directions.

The directivity index usually is a useful parameter only when the major lobe is somewhat narrow and the index is of the order of 10 dB or more. From Figure 3, Eq. (2) is clearly a very good approximation for

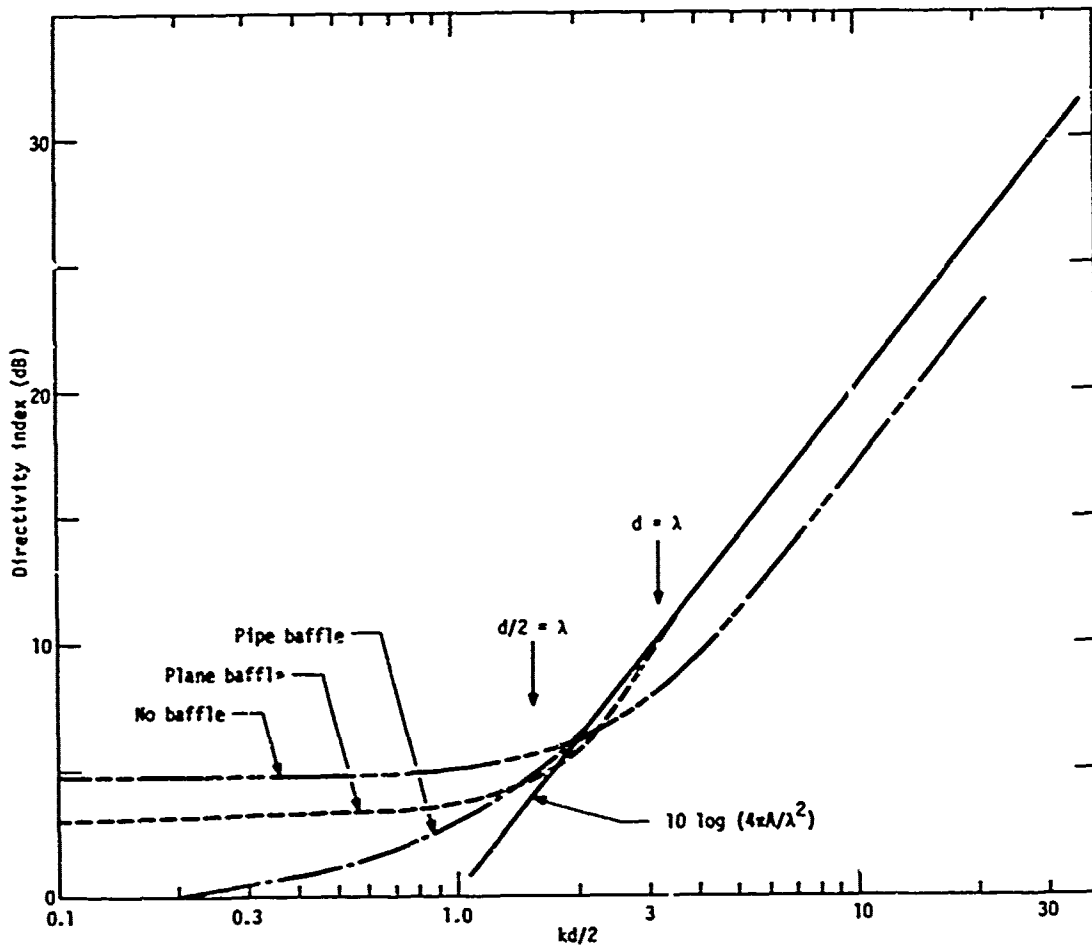


Fig. 3. The directivity index of a circular piston of diameter d without baffle, with a rigid plane baffle, in the end of an infinitely long rigid pipe, and as approximated by the expression $10 \log (4\pi A/\lambda^2)$.

diameters of several wavelengths with either type of baffle, and even with no baffle if the 3-dB correction is subtracted. The lower limit of the approximation, for baffled pistons, is $d = \lambda$ for errors less than 0.1 dB, and $d/2 > \lambda$ for errors less than 1.0 dB.

Rectangular and Other Pistons

Theoretical values for the directivity index of rectangular pistons in infinite plane rigid baffles have been calculated by both Stenzel [1] and Molloy [2]. Stenzel [17] has pointed out some errors in Molloy's paper, so Stenzel's values have been used in preparing Fig. 4 whenever the two authors disagree. The approximation based on the area of the rectangle

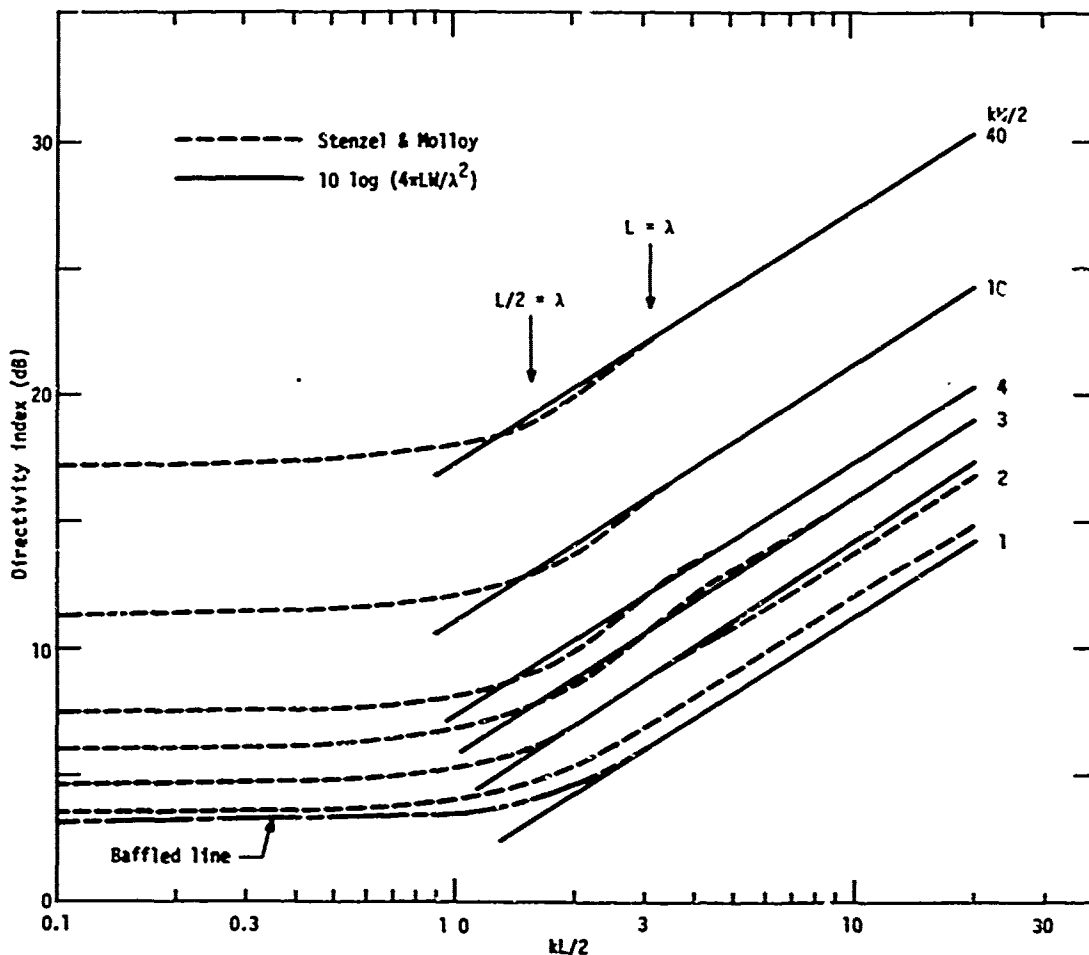


Fig. 4. The directivity index of a rectangular piston in an infinite plane rigid baffle as a function of length L or width W . Solid lines: as determined from the approximation based on area [$D_i = 10 \log (4\pi LW/\lambda^2)$]. Dashed lines: taken from data by Stenzel or Molloy. Dash-dot line: from Stenzel, after applying a 3-dB correction for a baffled line radiating into a half-space.

is also shown in Fig. 4. From these data, it is apparent that the limits for the approximation are at least as low as for the circular piston. That is, where both L and W equal or exceed a wavelength, or $kL/\lambda \geq \pi$ and $kW/\lambda \geq \pi$, the approximation error is negligible. And where both L and W equal or exceed a half wavelength, the error is less than 1.0 dB. It is interesting to note that when $kW/2 = 1$ or $W/\lambda = 1/\pi$, the approximation $4\pi A/\lambda^2$ reduces to $4L/\lambda$, or the approximation for a line source in a baffle radiating into a half-space.

It is evident from Figs. 3 and 4 that a baffled piston of any shape intermediate between a circle and rectangle (ellipse, octagon, etc.) would have a directivity index accurately given by $10 \log 4\pi A/\lambda^2$, provided that its smallest dimension is one wavelength. It is also evident that for dimensions greater than a wavelength, the baffle configuration makes no difference. Further, the directivity index of a piston of some unusual shape (a cross, for example) also is given by $10 \log 4\pi A/\lambda^2$, provided that its narrowest dimension exceeds a wavelength. This result follows from the argument that if the piston area is subdivided into segments, and the dimensions of each individual segment meet the wavelength criteria, then the whole radiator meets the approximation criterion.

Radiating Areas

Given that Eq. (2) is a valid theoretical approximation for most piston transducers, there still remains the problem of determining the piston area A in real transducers as illustrated by Fig. 1. It is a rule of thumb in sonar transducer design that if the element spacing in an array does not exceed 0.8λ , the array then functions essentially as a plane radiator. Insofar as the directivity pattern is concerned, this means that the major lobe of the array is the same as if the array were a uniform plane. The minor lobes, however, are quite different until the spacing becomes less than 0.2λ [18]. The use of the 0.8λ rule is amply supported by the implication from Table 1 that deviations in the minor lobes can be neglected for purposes of determining radiated energy.

Within the limit of the 0.8λ rule, the interstitial spaces in an array are included in the theoretical radiating area.

The periphery of the array is more of a problem. It would seem logical that half an interstitial space completely surrounding each element should be included in the area. This adds a thin peripheral area that, in the case of the F33 shown in Fig. 1b, is a uniform thin border a half-interstitial-space wide. But for the F27, shown in Fig. 1a, it is not so straightforward because of the unusual shape of the interstice. Further, if the interstices are included in the area, why not some of the concave corners at the periphery? Calculations of the effective areas of the F27 and F33 were made in various ways, including subjective judgements in some cases. The results showed a spread of about 10% in the area, or 0.5 dB in the directivity index. An area determined by averaging the results of several techniques is probably the only practical method.

Beam Widths

The effective area of a piston can be found by measuring the beam width of the major lobe in the pattern, provided the area is or approximates a circle, square, or rectangle.

The diameter-to-wavelength ratio d/λ of a circular piston is given in terms of the 6-dB-down half beam width θ by

$$d/\lambda = 0.70/\sin \theta. \quad (3)$$

Similarly, the side of a square or rectangle, or the length of a line, is given by

$$L/\lambda = 0.60/\sin \theta, \quad (4)$$

where θ is the 6-dB-down half beam width of the pattern in the plane of the dimension L .

The directivity index then is found from the dimensions and Eq. (2).

This method has the advantage of dealing directly with the radiated acoustic energy. The disadvantage is that most transducers do not have ideal shapes, as--for example--the F27 and F33, and beam widths in several planes must be averaged. This was done for the data shown for method 2 in Fig. 2. The results in Fig. 2 indicate that averaging beam widths produces about the same results as averaging areas.

Beam widths are measured at either the 3-, 6-, or 10-dB-down points. It was found that using the 6- and 10-dB down values for θ in Eqs. (3) and (4) produced the most consistent results, though using the 3-dB-down beam width produced directivity indexes only 0.1 or 0.2 dB different from the other two. It probably is best to measure all three beam widths and check against the theoretical values that show the relative beam widths as

3 dB down	0.73
6 dB down	1.00
10 dB down	1.23

These ratios apply to both circular pistons and square or rectangular pistons (and lines) in planes parallel to a side.

The fact that the ratios are the same for both illustrates that the two-dimensional patterns have the same relative shape in the direction where most of the sound energy is radiated.

Rear Lobes

Perhaps the most consistent difference between the patterns of real and ideal piston transducers is in the existence of rear lobes. Ideally, there would be no rear lobes. In practice, they appear often because it is so difficult to obtain a truly rigid baffle or housing in underwater acoustics.

If the rear or back plate of a transducer housing vibrates, a pattern lobe will appear at 180°. The rear lobe usually is slightly narrower than the front or major lobe because the back plate is larger than the array or diaphragm designed to radiate in the forward direction. If one assumes conservatively that the rear lobe has the same beam width as the major lobe, then a correction to the directivity index from Eq. (2) is easily estimated from the number of decibels that the rear lobe is below the major lobe. Such corrections are shown in Table 2. Minor lobes to the rear at angles other than 180° usually are small enough to neglect.

Table 2. Correction (in decibels) to calculated directivity index as a function of rear lobe height.

Rear lobe down (dB)	D_i correction (dB)
10.0	-0.4
12.5	-0.3
15.0	-0.2
17.5	-0.1
20.0	<-0.1

Radiation Resistance

The relationship between the radiation resistance R and the directivity factor R_θ of a baffled piston can be useful in ascertaining the limit of validity of Eq. (2).

The diffraction constant D of any transducer is given by [19]

$$D^2 = RR_\theta [4\pi / (k^2 \rho c)], \quad (5)$$

where R is the radiation resistance in acoustical ohms. Equation (5) can be written

$$R_\theta = (D^2 \pi / \lambda^2) (\rho c / R). \quad (6)$$

For a piston in a rigid baffle, $D = 2$, and when the piston is large, $R = \rho c / A$ and the acoustic load becomes largely resistive. Then Eq. (6) becomes,

$$R_\theta = 4\pi A / \lambda^2, \quad (7)$$

or the equivalent of Eq. (2). Thus, Eqs. (2) and (7) are valid approximations whenever a baffled transducer has a specific acoustic impedance load of ρc .

Equation (6) can also be used for other transducer configurations, where R is available from a number of books and D is available from Henriquez's paper [20].

Line Sources

The theoretical values of the directivity index of line sources have been well known from the work of Stenzel [1] and Molloy [2]. However, the analysis or calculations of both authors have been marred by errors. Stenzel [17] has pointed out some errors in Molloy's paper [2]. Stenzel, in turn, has erred in his original work, and both a second edition by Erosze [12] and translations into English [10,11] contain additional errors. None of these latter errors are significant, but a resumé and correction seem in order.

Thirty years ago, the terminology was not consistent between "directivity" and "radiation," and between "factor" and "index." Also, by whatever name, the directivity factor was the reciprocal of the modern parameter. Consequently, in what follows, the current definition of directivity factor and appropriate inversions will be used.

The exact expression for the directivity factor R_θ of a line source is given in all sources as equivalent to

$$R_\theta^{-1} = -\frac{\sin^2(kL/2)}{(kL/2)^2} + \frac{2}{kL} \int_0^{kL} \frac{\sin t}{t} dt, \quad (8)$$

where k is the wave number and L the length of the line. Stenzel [1] derived Eq. (8) from the case of a rectangular piston in an infinite rigid baffle (but radiating on both sides of the baffle) letting the width of the rectangle approach zero.

Stenzel evaluated Eq. (8) numerically by using tables for the sine integral, and analytically by using the approximation for a sine integral

$$\int_0^x \frac{\sin t}{t} dt = \frac{\pi}{2} - \frac{\cos x}{x} \left(1 - \frac{2}{x^2} \right) - \frac{\sin x}{x}. \quad (9)$$

Substituting this approximation in Eq. (8), using trigometric identities for double angles, and rearranging, produces

$$R_\theta^{-1} = \frac{1}{kL} \left(\pi - \frac{2}{kL} - \frac{2 \sin kL}{kL} + \frac{4 \cos kL}{(kL)^3} \right). \quad (10)$$

Stenzel appears to have used the limit $x = kL/2$ instead of $x = 2(kL/2)$ with the result that the third and fourth terms in the parentheses in Eq. (10) are given incorrectly by him. Mongan's translation [10] and Brosze's second edition [12] follow neither Eq. (10) nor Stenzel's original Eq. (71). Stickley's translation [11] faithfully followed Stenzel, but later someone found the original error and added a footnote resulting in Eq. (10). The American Standard [24] has used Stickley's corrected translation in its Eq. (72).

If one examines how good an approximation Eq. (10) is for Eq. (8), a surprising conclusion emerges. Figure 5 shows a plot of the exact expression, Eq. (8), together with approximations using one, two, or all four terms of Eq. (10). The three-term approximation is not shown because it is essentially the same as the four-term for $kL/\lambda > 2$, and like the four-term is very different from the others for $kL/\lambda < 2$.

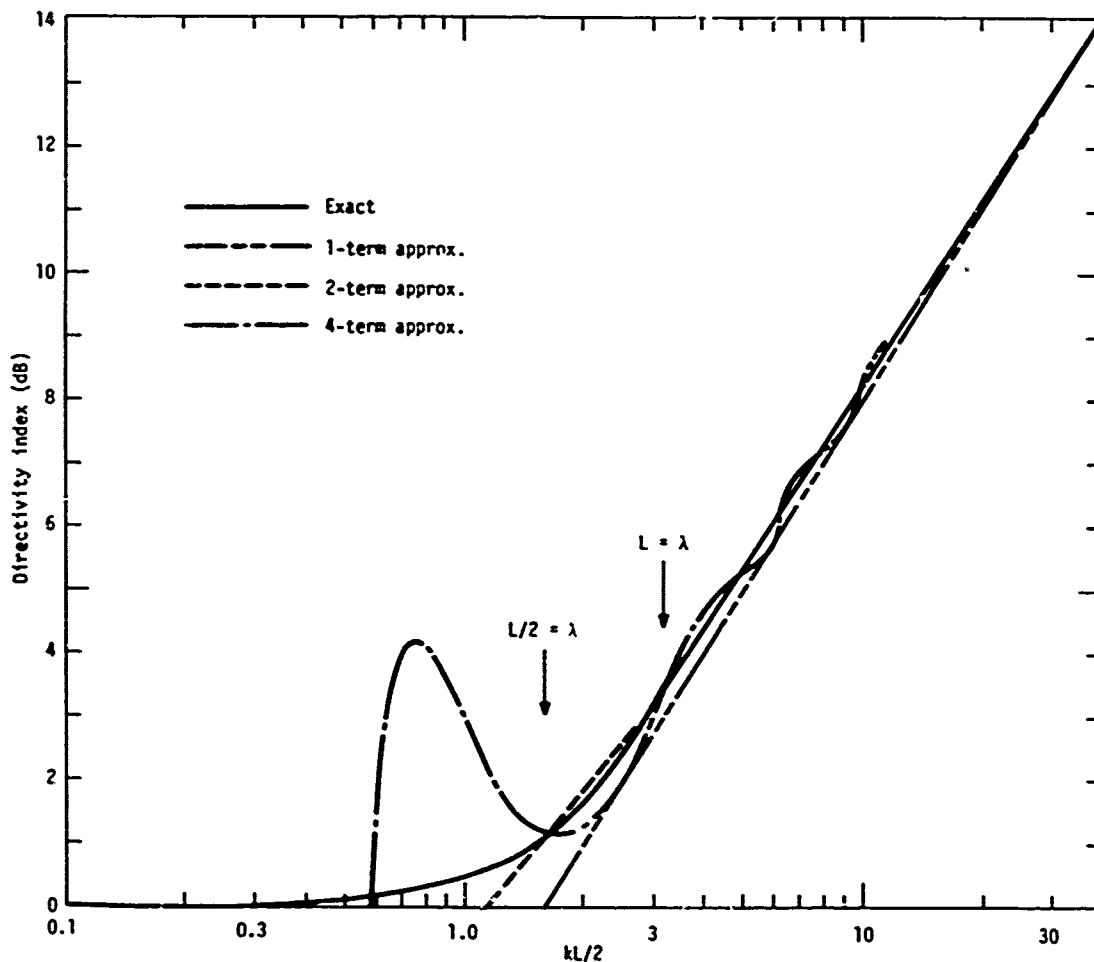


Fig. 5. The directivity index of a line source according to Stenzel's exact expression (Eq. (8)), and three degrees of approximation by Eq. (10).

It should be noted that the vertical scale in Fig. 5 is half that of Figs. 3 and 4, so as to show the differences among the various approximations.

Clearly the four terms are a poorer approximation than the two terms, and the two trigonometric terms and the errors in them can be neglected.

The one-term approximation,

$$R_{\theta} = kL/\pi = 2L/\lambda \quad (11)$$

is commonly used in transducer analysis, but at low frequencies or for short lines the two terms,

$$R_{\theta} = \left(\frac{\pi}{kL} - \frac{2}{(kL)^2} \right)^{-1} = \frac{2L}{\lambda} \left(1 - \frac{\lambda}{\pi^2 L} \right)^{-1} \quad (12)$$

should be used.

In terms of the directivity index $D_i = 10 \log R_{\theta}$, the errors are

$$\left. \begin{array}{l} <0.5 \text{ dB for } L > 0.9\lambda \\ <0.2 \text{ dB for } L > 2.0\lambda \end{array} \right\} \text{ for } R_{\theta} = 2L/\lambda$$

$$<0.2 \text{ dB for } L > 0.5\lambda \quad \text{for } R_{\theta} = (2L/\lambda) (1 - \lambda/\pi^2 L)^{-1}$$

The line transducer has no baffle conditions or rear lobes to be concerned with. The length L is determined from beam widths exactly as the length of a rectangular piston; or from the known physical length that includes a half-interstitial space at each end.

Shaded Transducers

All of the foregoing approximation theory is based on the cases of pistons or lines that have uniform response over the entire area or length. Many sonar transducers are *shaded*. That is, the vibration amplitude, when transmitting, is a maximum at the center and tapers off to some lower values toward the periphery or end. The purpose is to suppress the side lobes, but an associated effect is to widen the major lobe. Can the approximations for uniform radiators be applied to shaded transducers?

The effect of suppressing the minor lobes can be estimated from Table 1. In the most extreme case of a piston pattern with no minor lobes, the maximum correction is 16%, or a 0.6-dB increase in the directivity index of a corresponding uniform piston. For a shaded line, the maximum correction is a 0.3-dB addition. Other corrections can be estimated within very small errors.

The widening of the major lobe reduces to the question of whether the relative shape of the lobe remains the same, or whether the major lobe

approximates that radiated from a smaller uniform source. In addressing these questions, two types of shading functions were investigated--where shading function pertains to the mathematical description of the sensitivity of a radiator as a function of the distance from the geometric center.

The first was a "linear taper," where the sensitivity varies linearly from the maximum at the center to zero at the end or periphery. The pattern of such a line is given by

$$P_{\theta} = \left[\frac{\sin [(\pi L/2\lambda) \sin \theta]}{(\pi L/2\lambda) \sin \theta} \right]^2. \quad (13)$$

The first minor lobe of this pattern is 26.6 dB down.

The second function is that for a "binomial line." This function is used with a line array of point elements whose sensitivities are proportional to the coefficients in the expansion of a binomial function

$(x + y)^{n-1}$, where n is the number of elements. If the element spacing is a half-wavelength, the shading is perfect or there are no minor lobes. For the investigation here, n was 10. The optimum half-wavelength spacing was used, thereby simulating a five-wavelength continuous line. The coefficients in the expansion of $(x + y)^9$ are 1, 9, 36, 84, 126, 126, 84, 36, 9, and 1. When normalized so that their sum is one, these coefficients become 0.002, 0.018, 0.070, 0.164, 0.246, 0.246, 0.164, 0.070, 0.018, and 0.002. The pattern of such a line array with half-wavelength spacing is given by

$$p = 2[0.246 \cos(0.5\pi \sin \theta) + 0.164 \cos(1.5\pi \sin \theta) + 0.070 \cos(2.5\pi \sin \theta) + 0.018 \cos(3.5\pi \sin \theta) + 0.002 \cos(4.5\pi \sin \theta)]. \quad (14)$$

The relative beam widths of the pattern of Eq. (14) are

3 dB down	0.70
6 dB down	1.00
10 dB down	1.23

Comparing these relative beam widths with those of uniform radiators, it is seen that the two cases are similar, but not identical.

To obtain a quantitative effect on the directivity index, a uniform line length and a linearly tapered line length were chosen so that their patterns had the same 6-dB-down beam width as the binomial line. These lengths turned out to be 2.4λ and 3.59λ , respectively. The major lobes of the three patterns are shown in Fig. 6.

Graphical calculation of the directivity index using the patterns shown as the major lobe of a line source (having a toroidal pattern), and neglecting all minor lobes, gives the following:

Uniform line	6.6 dB
Linearly tapered line	6.5 dB
Binomial line array	6.5 dB

The theoretical value for the uniform line is 6.9 dB for the whole pattern and 7.2 dB for only the major lobe. The 0.6-dB error in the graphical calculation is not unexpected in light of the data in Fig. 2 and the imprecision in measuring levels at angles near the pattern axis.

If the patterns in Fig. 6 are taken as those for a circular piston, the graphical calculations yields the following directivity indexes:

Uniform line	19.4 dB
Linearly tapered line	19.6 dB
Binomial line array	19.5 dB

The conclusion here is that the differences in the patterns of uniform and shaded radiators are less than measurement error insofar as the effect on the directivity index is concerned. Consequently, the technique of measuring the 6-dB-down beam width and then calculating the directivity index as if the transducer were uniform is acceptably accurate for shaded transducers.

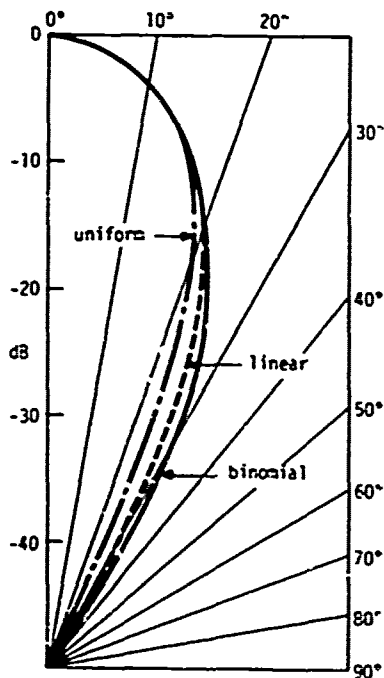


Fig. 6. Major lobes of patterns for a uniform line, a linearly tapered line, and 10-element binomially shaded line array.

Arrays with Mutual Coupling

One other case of nonuniform radiators should be mentioned. In large low-frequency arrays where the element spacing is a small fraction of a

wavelength, there is mutual interaction or coupling among the elements. That is, the radiation impedance of one element is affected by the vibration of neighboring elements. The elements usually are vibrating at their resonance frequency and thus are sensitive to any effect on their radiation impedance. The result can be nonuniform vibration among the elements due to this mutual coupling, which would invalidate the directivity index computation based on uniform pistons or lines. As in the case of shaded transducers, it becomes a question of whether the measured pattern is similar enough to that of an equivalent uniform array. Unlike shading, mutual coupling is an unintentional and undesirable effect. When a pattern is significantly affected by mutual coupling, the problem usually is that of correcting the cause rather than measuring the result.

Conclusion

From both experiment and theory, it is apparent that the directivity index of any ordinary transducer can be obtained from calculations based on known configuration and dimensions or beam-width measurements with a degree of reliability and accuracy that is no worse than any measurement technique. A conservative limit for the validity of such calculations is that the minimum transducer dimension be one wavelength.

Acknowledgement

The author is indebted to James D. George for computer calculations used in this study.

References

- [1] H. Stenzel, *Leitfaden zur Berechnung von Schallvorgängen* (Julius Springer, Berlin, 1939); also republished by J. W. Edwards in 1944 in the United States under the authority of Alien Property Custodian License No. A-491.
- [2] C. T. Molloy, "Calculation of the Directivity Index for Various Types of Radiators," *J. Acoust. Soc. Am.* 20, 387-405 (1948).
- [3] P. M. Kendig and R. E. Mueser, "A Simplified Method for Determining Transducer Directivity Index," *J. Acoust. Soc. Am.* 19, 691-694 (1947).
- [4] C. E. Green and J. R. Roshon, "Directivity Factor Computer for Electroacoustic Transducers," NEL Report 1196, U. S. Navy Electronics Laboratory, San Diego, California, 13 Sep 1963.

- [5] Scientific-Atlanta, Inc. is the manufacturer of equipment for integrating the patterns of both sonar transducers and antennas.
- [6] A. M. Young, "Digital System for the Measurement of Directivity Index," NRL Report 7585, 20 Apr 1973 [AD-758 639].
- [7] R. F. Green, "Measuring the Directivity Index of Underwater Sound Projectors," IEEE Trans. on Audio and Electroacoustics AU-21, 407-412 (1973).
- [8] R. J. Bobber, *Underwater Electroacoustic Measurements* (Naval Research Laboratory, U. S. Government Printing Office, Washington, D. C., 1970), pp. 83-90.
- [9] Special slide rules for calculating sonar transducer parameters have been produced by the Edo Corporation, Sperry-Rand, and The Raytheon Corp.
- [10] H. Stenzel, *Guide for the Calculation of Sound Processes*, NAVSHIPS 250-940; translation of reference 1 by C. E. Mongan, Jr., May 1947.
- [11] H. Stenzel, *Handbook for the Calculation of Sound Propagation Phenomena*, NRL Translation 130 by A. R. Stickley, Nov 1947 [translation of reference 1 into English].
- [12] H. Stenzel and O. Brosze, *Leitfaden zur Berechnung von Schallvorgängen*, Zweite Auflage (Springer-Verlag, Berlin, 1958) [a second edition of reference 1, in German, by Brosze after Stenzel's death].
- [13] Reference 8, pp. 89-90.
- [14] B. G. Watters, "A Reverberant Tank for Underwater Measurements," J. Acoust. Soc. Am. 53, 357(A) (1973) [Paper II4, 84th Meeting of the Acoustical Society of America, Nov 1972].
- [15] A. E. Reznikov and A. Ya. Snytko, "Problem of Measuring the Axial Concentration Coefficient in Ultrasonic Radiators," Measurement Techniques [the Soviet Journal *Izmeritel'naya Tekhnika* in English translation], No. 7, July 1965, pp. 654-657.
- [16] L. L. Beranek, *Acoustics* (McGraw-Hill Book Co., New York, 1954), p. 112.
- [17] H. Stenzel, "Remarks on a Paper entitled 'Calculation of the Directivity Index for Various Types of Radiators,'" J. Acoust. Soc. Am. 24, 417-418 (1952).
- [18] R. J. Bobber, "The Effects of Element Packing on the Complete Radiation Patterns of Arrays," NRL Memorandum Report 2206, 18 Jan 1971 [AD-718 312].
- [19] R. J. Bobber, "Diffraction Constants of Transducers," J. Acoust. Soc. Am. 37, 591-595 (1965).
- [20] T. A. Henriquez, "Diffraction Constants of Acoustic Transducers," J. Acoust. Soc. Am. 36, 267-269 (1964).
- [21] American National Standard, "Procedures for Calibration of Underwater Electroacoustic Transducers," ANSI S1.20-1972, p. 27.